Optical characterisation of apple tissue: a multiscale approach

W. Saeys,[a] S. N. Thennadil,[b] H. Ramon[a] and B. Nicolaï[b]

[a]*BIOSYST-MeBioS K.U.Leuven, Kasteelpark Arenberg 30, 3001 Leuven, Belgium. E-mail: wouter.saeys@biw.kuleuven.be*

[b]*Chemical and Process Engineering, University of Strathclyde, 75 Montrose Street, Glasgow G1 1XJ, United Kingdom*

Introduction

The change of Vis/NIR radiation when propagating through fruit tissue is the result of a complex process of molecule-specific absorptions and multiple light scattering, caused by the interaction of photons with the microstructure. Photons are most strongly scattered by those structures whose size matches the photon wavelength (0.4–2.5 μm). In biological tissue these are cell organelles like nuclei, mitochondria, vesicles, membranes and cell walls.[1] Although several data pre-treatment methods have been developed to reduce the effect of light scattering on the relation between the measured spectrum and the chemical concentrations,[2] variations in the microstructure still often lead to deviations in the predicted concentrations which demand recalibration. Moreover, these microstructure properties determine the physical properties of fruit tissue, such as firmness, which are also of interest.[3] In addition, intact fruit are characterised by a layered structure (skin and flesh). Therefore, novel measurement techniques and a novel modeling paradigm are needed to obtain maximum benefit from the potential of NIR spectroscopy for the characterisation of complex biological tissues, like fruits. In this study, a multiscale approach has been applied to model the light propagation in apple tissue.

Theory

First, an apple is modeled at the *mesoscale* (tissue layers ~mm) as two uniform layers: the skin and the flesh, where the light propagation in each layer is defined by three bulk properties: the absorption coefficient μ_a, the transport scattering coefficient μ_s' and the phase function $\rho(\theta)$. Using these three bulk properties the reflectance and transmittance spectra of these layers can be simulated using the radiative transport equation. Since these bulk optical properties cannot be measured directly, unlike the transmittance and reflectance spectra, they have to be estimated iteratively by a so-called inverse light propagation algorithm.[4]

In a second step, the estimated scattering and absorption properties are then related to the chemical composition and microstructure of the skin and flesh. For both layers, the absorption coefficient μ_a can then be modeled on the *chemical level* based on the multi-component Beer's law. The transport scattering coefficient μ_s', which describes which portion of the incident light is

scattered is then modeled at the *microscale* as a set of spheres using Mie theory to extract information on the size and density of the scatterers, using the following equation:[5]

$$\mu_S' \approx ax^b = a\left(\frac{2\pi r_e n}{\lambda}\right)^b = c\lambda^{-b} \quad (1)$$

where a is a function of the density of the scatterers, b is proportional to the size of the scatterers, n is the refractive index of the scatterers, λ is the wavelength and r_e is the radius of the equivalent spherical scatterers. This *microscale* model thus describes the transport scattering coefficient μ_s' as an exponentially decreasing function of the wavelength, a feature which has also been reported for other biological tissues.[6] Information on the microscale properties of the tissue can thus be extracted from the estimated bulk scattering coefficient spectra $\mu_s'(\lambda)$ by fitting a decreasing exponential to it to find the coefficients c and b. However, the radius of the equivalent spherical scatterers r_e and the density parameter a cannot be directly derived from coefficients b and c, because both b and c are functions of the size of the scatterers. Therefore, we derive r_e from b using Nilsson's equation:[7]

$$\begin{aligned} b &= 1109.5\ r_e^3 - 341.67\ r_e^2 + 9.3696\ r_e + 3.9359 \text{ for } r_e < 0.23\mu m \\ b &= -23.909\ r_e^3 + 37.218\ r_e^2 - 19.534\ r_e + 3.965 \text{ if } 0.2 < r_e \leq 2\mu m \end{aligned} \quad (2)$$

and substitute this r_e into Eqn (1) to calculate the density parameter a.

Experimental

Forty-two apples of three different cultivars (Royal Gala, Granny Smith and Braeburn) were purchased and stored under room temperature for 1 to 21 days. On each of the 9 measurement days skin and flesh tissue samples from 1 or 2 apples per cultivar were isolated and placed between glass slabs for spectral measurement. From each of these tissue samples the diffuse reflectance, the diffuse transmittance and the collimated transmittance were measured in the 350 to 2500 nm range using a Varian Cary 5000 spectrophotometer equipped with an external diffuse reflectance accessory.

From the measured transmittance and reflectance spectra, the bulk optical properties were estimated using an inverse adding-doubling algorithm.[4] For each skin and flesh tissue sample the density parameter a and the radius r_e of the equivalent spherical scatterers was then estimated using the procedure described above. The refractive index value in Eqn (1) was set at the average value of 1.35. Finally, the effects of tissue type, cultivar, apple size and shelflife on the size and density of the equivalent scatterers were investigated with an analysis of variance.

Results and discussion

The estimated absorption coefficient μ_a spectra (Figure 1) are dominated by absorption by water in the NIR region (especially at 1450 and 1900 nm) and by pigments and chlorophyll (at 675 nm) in the visible region.

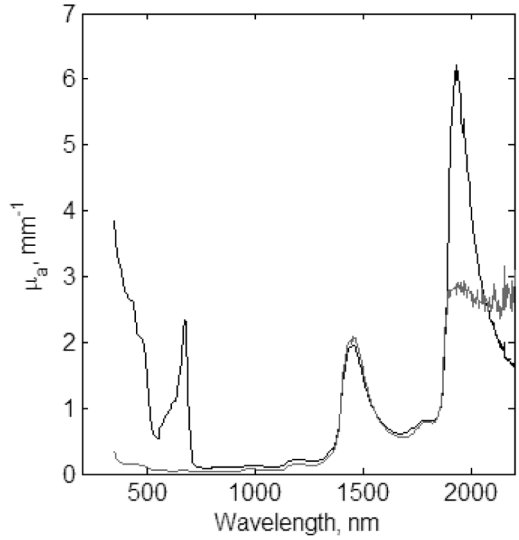

Figure 1. Average absorbance coefficient spectra $\mu_a(\lambda)$ for Granny Smith apple skin (black) and flesh (grey) tissue.

The concentration of chlorophyll was found to be much higher in skin tissue than in flesh tissue. The estimated transport scattering coefficient μ_s' spectra (Figure 2) were found to follow the decreasing exponential function with increasing wavelength very well.

However, peaks in the μ_s' spectra were observed at the same wavelength regions as the peaks in the μ_a spectra. These peaks cannot be explained by light scattering, but are most likely

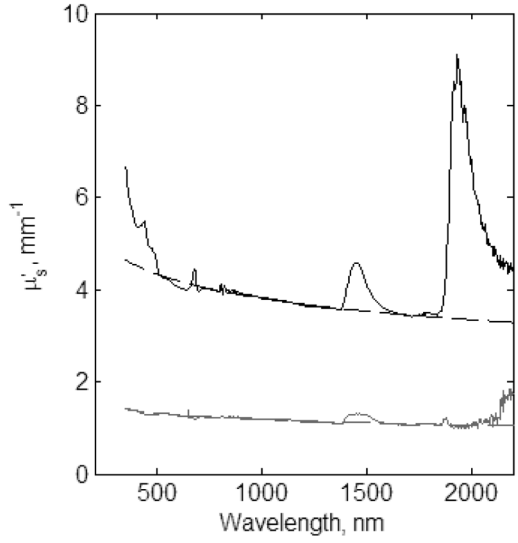

Figure 2. Measured (solid) and simulated (dashed) average transport scattering coefficient spectra $\mu_s'(\lambda)$ for Granny Smith apple skin (black) and flesh (grey) tissue.

Table 1. Estimated microscale properties for apple skin and flesh tissue.

	a (mm^{-1})		r_e (μm)	
	Skin	Flesh	Skin	Flesh
Gala	2.17 ± 0.361	0.98 ± 0.348	0.72 ± 0.025	0.77 ± 0.060
Granny Smith	2.63 ± 0.500	0.89 ± 0.280	0.74 ± 0.019	0.76 ± 0.068
Braeburn	2.30 ± 0.628	0.84 ± 0.246	0.73 ± 0.024	0.75 ± 0.050

'cross-talk' between μ_a and μ_s' caused by ill-conditioning of the inverse estimation, due to the low signal to noise ratio of the small transmittance signals acquired at these absorption peaks. Therefore, these regions of high absorbance were not taken into account when estimating the scatter function coefficients *b* and *c*. It was also observed that apple skin tissue is around three times more scattering than the corresponding flesh tissue. Through the *microscale* modelling this difference could be attributed to a higher density of the scatterers in the lightpath *a* and a slightly smaller equivalent radius of the scatterers r_e (Table 1).

From Table 1 it can also be seen that the different cultivars have different average densities and radii of the equivalent spherical scatterers of their skin and flesh. However, only the difference in density and radii of the scatterers of Gala and Granny Smith skin tissue was found to be significant, due to the large variation in scattering properties of apples from the same cultivar.

From this study, it can be concluded that the optical properties of apple skin and flesh are so different, that we should not consider these as one homogeneous bulk layer, as is traditionally done in vis-NIR spectroscopy of intact apples or other fruit.

References

1. A. Kienle, R. Michels, J. Schäfer and O. Fugger, in: *Advances in Medical Engineering* Ed by T.M. Buzug, D. Holz, J. Bongartz, M. Kohl-Bareis, U. Hartzmann and S. Weber. Springer, Berlin-Heidelberg, Germany, p, 355 (2008).
2. S. N. Thennadil, H. Martens and A. Kohler, *Appl. Spectrosc.* **3,** 315 (2006).
3. E. Bobelyn, A.-S. Serban, M. Nicu, J. Lammertyn, B.M. Nicolai and W. Saeys, *Postharvest Biol. Technol.* **55,** 133 (2010).
4. W. Saeys, M.A. Velazco-Roa, S.N. Thennadil, H. Ramon and B.M. Nicolai, *Appl. Opt.* **47,** 908 (2008).
5. R. Cubeddu, C. D'Andrea, A. Pifferi, P. Taroni, A. Torricelli, C. Valentini, C. Dover, D. Johnson, M. Ruiz-Altisent and C. Valero, *Appl. Opt.* **40,** 538 (2001).
6. A.N. Bashkatov, E.A. Gerina, V.I. Kochubey and V.V. Tuchin, *Opt. Spectrosc.* **99,** 836 (2005).
7. A.M.K. Nilsson, C. Sturesson, D.L. Liu and S. Andersson-Engels, *Appl. Opt.* **37,** 1256 (1998).